Order-Disorder Transition during Approach and Separation of Two Parallel Surfaces

S. Karaborni

Koninklijke/Shell-Laboratorium, Amsterdam (Shell Research BV), P.O. Box 38000, 1030 BN Amsterdam, The Netherlands

(Received 31 January 1994)

The molecular dynamics technique is used to investigate the effect of the approach and separation of two monolayers on the dynamics, structure, and chain conformation within each layer, and the total internal energy. The results show that at certain distances between the monolayers there is a strong increase in ordering, and that the internal energy during approach is consistently different from that during separation. Hysteresis effects in these simulations appear to be due to an order-disorder transition and not to chain entanglements between the monolayers.

PACS numbers: 68.35.Wm, 68.35.Rh, 68.55.Jk, 81.30.Hd

Two monolayers whose amphiphilic tails are adjacent to each other form a system of central importance in many applications. Applications of bilayers span the field of biology, colloid stability, and tribology. In several products, such as lubricating oils and diesel fuels, amphiphilic molecules adsorbed at the surfaces of colloid particles induce a modification in stability upon contact of the two monolayers by providing a steric repulsion between the particles [1]. In other applications, such as in computer disk lubrication, adjacent amphiphilic monolayers are being investigated for use in decreasing friction [2,3] between two moving plates by modifying the well-known stick and slip cycle [3].

In some adhesion experiments, the structures of surfactant monolayers are being investigated to determine the origin of the well-known hysteresis during loading-unloading cycles [4,5]. Israelachvili and co-workers contend that hysteresis effects are due to entanglements or interdigitation between the amphiphilic molecules from both monolayers [4–6]. In their analysis they argue that since entanglements are much easier than disentaglements in the amorphous state, the required energy to separate the monolayers is much more than that during loading. On the other hand, Chaudhury and Owen reported hysteresis in adhesion experiments even for very dense monolayers in which entanglements are very unlikely [7]. Clearly, a better understanding of hysteresis effects in loading-unloading experiments could contribute to a better design of additive layers in adhesion, nanolubrication, and colloid stability.

In addition to the technological use of two-layer systems, their behavior is of fundamental importance in determining the origin of difference between the behavior of two-layer systems, and that of the well-studied single monolayer systems [8]. In the work described here we use the molecular dynamics (MD) technique to gain a better understanding of phenomena that occur during approach-separation experiments by studying the dynamics, structure, and conformation within amphiphilic monolayers which collide with and separate from each other.

The molecule studied contains 19 segments having the same size and energy characteristics as CH_2 groups [9], and a head group that has the same size and energy parameters as a carboxylate group [10]. All interactions were treated on the molecular level except plate-amphiphile interactions, which were modeled using a Lennard-Jones (3-9) potential [11]. The energy parameters in the external potentials were chosen such that the head groups are strongly bound to the solid surfaces. The pseudoatoms of the amphiphilic molecules interact via an anisotropic united atom model [9] that accounts implicitly for the presence of hydrogens in real systems.

A series of molecular dynamics simulations was performed for amphiphilic chains at an average coverage on each plate of 25 $Å^2$/molecule, which is roughly the same coverage as that used by Israelachvili. The simulations were performed for 128 molecules equally divided between the two plates, and periodically replicated in the x and y directions. The temperature was 298 K. The simulations were performed by periodically decreasing the distance between the two plates in steps not higher than 0.2σ ($\sigma = 3.527$ Å). After periods of less than 10 psec, in which equilibration measures such as *trans* fraction values were satisfied, average production runs of 5 to 20 psec were performed, and then stored at intervals of 0.1 psec for further analysis. In total 40 distances were sampled. The average compression rate used in these simulations, which is approximately 7 ms^{-1}, is slightly lower than that used by Luedtke and Landman to model an atomic force microscope (AFM) tip approaching a film of n-hexadecane (16.7 ms^{-1}) [12]. Since it is presently unclear how experimental compression rates should be scaled to simulation values, we used compression rates that are low enough to allow for equilibration of the *trans* fraction between two successive compressions. Prior simulations on dense surfactant monolayers showed that the equilibration of the *trans* fraction controls the relaxation of the monolayers [13].

A series of analyses has been used to investigate the effect of distance between the two monolayers on conformations, structural, and dynamic properties. The

 0031-9007/94/73(12)/1668(4)$06.00

properties calculated were the average number of dihedral angles which are in *trans* conformation, the average tilt angle, the transverse structure factors, and the relaxation rates of the molecular reorientation within the monolayers.

One of the most significant measures of chain conformation is the average *trans* fraction, which is defined as the number of dihedral angles in *trans* conformation divided by the total number of dihedral angles. Figure 1(a) is a plot of the average *trans* fraction as a function of the average distance between the end-methyl groups from the two monolayers (hereafter the interlayer distance Z). This curve clearly shows that the *trans* fraction increases drastically from 0.92 at large distances to approximately 0.99 at intermediate distances. This increase in chain *trans* fraction results in a straightening of the chains. Eventually, as the distance between the monolayers becomes very small, the *trans* fraction decreases due to the formation of gauche defects in the headgroup regions (near the solid surfaces). A similar decrease in average *trans* fraction is seen when an AFM tip approaches a self-assembled monolayer [14]. The high fraction of *trans* angles at the intermediate distance is highly indicative of an ordered crystalline state. Such high fractions are only seen in the highest density phases of Langmuir and Langmuir-Blodgett monolayers which correspond to ≈ 20 Å^2/molecule or less [11,15]. At coverage similar to that used in these simulations the *trans* fraction in monolayers is much lower [11,15].

Figure 1(b) shows the behavior of the average tilt angle as a function of the interlayer distance. At large distances, the tilt angle is approximately 30°, which is in agreement with the tilt angle measured by x-ray reflection of fatty acid monolayers at similar surface density [16]. As the molecules from the two monolayers begin to feel each other, the tilt angle increases due to the decrease in the gauche defects in the midsections of both monolayers. A similar coupling between tilt angle and gauche defects has been noted by Buontempo *et al.* [13] in Langmuir monolayers of long-chain alcohols. At very small distances, the tilt angle continues to increase although the average *trans* fraction is decreasing. This increase in tilt angle is due to the formation of gauche defects near the headgroup region. The increase in tilt angle causes a decrease in the average height of the two approaching monolayers.

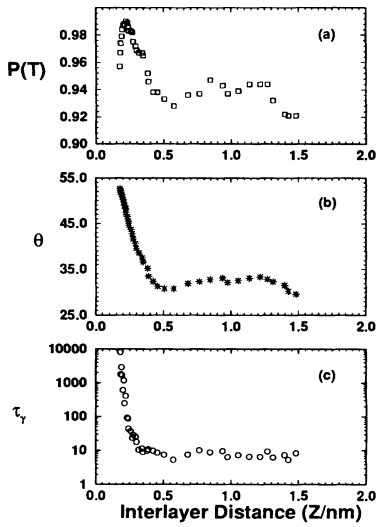

FIG. 1. Average properties during approach, as a function of the average interlayer distance Z. (a) Average *trans* function $P(T)$, (b) average tilt angle θ in degrees, (c) relaxation time τ_γ of the time autocorrelation function $\gamma(t)$. τ_γ is in picoseconds.

We have also investigated the dynamic properties of the monolayers by calculating the rate of reorientation of molecules around their major axes. The reorientation of the molecules around their major axes is calculated using a time autocorrelation function. The relaxation times, τ_γ, are then determined by fitting the correlation functions to exponential functions [15,17]. In Fig. 1(c), τ_γ is plotted as a function of the average interlayer distance. At large distances τ_γ is ≈ 8 psec. As the distance is decreased, τ_γ increases, reaching a value that is 2 to 3 orders of magnitude higher than the value at large distances. The relaxation time at large distance is similar to the relaxation time in the rotator phase of n-alkanes [18,19], and the relaxation time in the rotator phase of a model n-alkyl thiol monolayer [17], and model Langmuir monolayers [15]. By analogy with crystal alkanes, the monolayer at large distances must also be in a free rotator phase. As the friction between neighboring molecules increases, so does the relaxation time at short plate distance. At very short distances the two monolayers must be in a nonrotator or small oscillation phase.

A good measure of lattice order-disorder is the structure factor. In Fig. 2, plots are shown of the two-dimensional structure factors in both monolayers at two average interlayer distances. The usual peak at the origin, whose height is equal to the number of pseudoatoms, is not shown. The two plots show a clear dependence of peak heights and widths on interlayer distance. On average the peaks are approximately 10 times higher at the small distance than at the large distance. At the large distance all six peaks are present. (In reality there are only three independent peaks; the remaining three are due to symmetry of the structure factors about the origin.) Because of tilting in the monolayers, four of the peaks are higher than the remaining two. It is important to note that secondary peaks are also present. This fact, together with the absence of a connecting ring between the primary peaks, indicates that the monolayers are not in a true liquid state, and are most likely in a low symmetry crystalline phase. At the small distance there are two high peaks in each monolayer, indicating the presence of a well-defined monolayer tilt. Figure 3 shows the monolayers at a large and an intermediate separation.

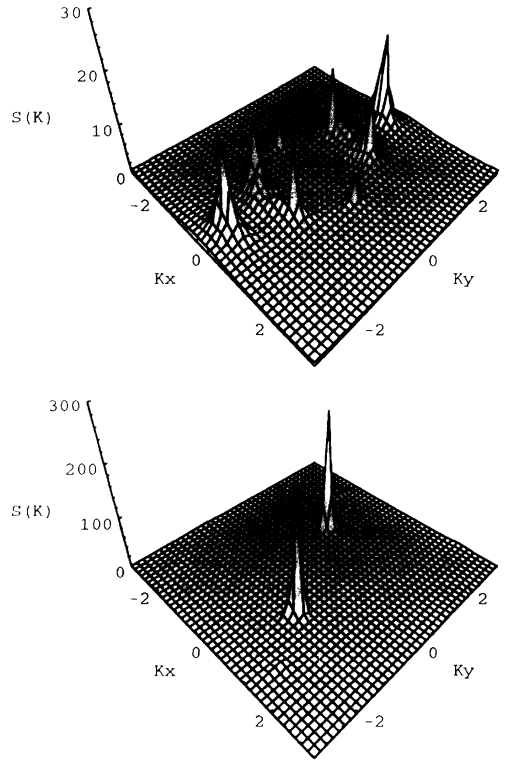

FIG. 2. Average transverse structure factors at two average interlayer distances. Top: $Z = 1.24$ nm. Bottom: $Z = 0.20$ nm.

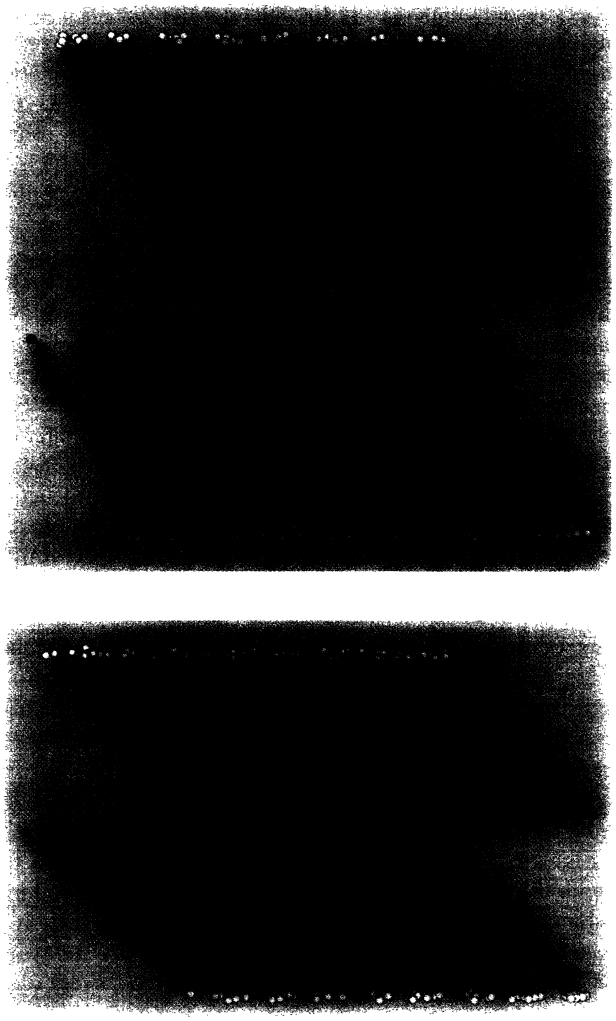

FIG. 3. Snapshots of the system at two interlayer distances: top: $Z = 0.938$ nm and bottom: $Z = 0.233$ nm. The headgroups are displayed in yellow and the methylene segments in green. Gauche defects separated from each other by more than one *trans* dihedral angle are displayed in red. Gauche defects separated from each other by exactly one *trans* dihedral angle (kink defects $g^{\pm}tg^{\mp}$) are displayed in blue.

Chain conformation, structure factors, and relaxation times indicate the presence of a transition from a liquid to a solid phase. The liquid phase is not amorphous, and has crystallinelike or hexaticlike order. This is mostly exhibited by the secondary peaks in the structure factor plots and the absence of a connecting ring in the same plots, as well as the relaxation rate of reorientation, which resembles that of the crystalline rotator phase of *n*-alkanes. The solid phase has long range positional, lattice orientational, and molecular tilt azimuthal order. This solid-crystalline phase is characterized by a high fraction of *trans* angles, very high structure factor peaks, large tilt angles, and a high relaxation rate of molecular reorientation.

We believe that the ordering phase transition is due to excluded volume effects. In other words, a decrease in the volume available for the molecules induces a better packing. This is accomplished via molecules that exclude their gauche defects in their midsections, and become aligned with each other such that all molecules have the same molecular tilt azimuthal angles. Note that the ordering transition begins when the average distance between the monolayer tips is ≈ 0.47 nm ($\sigma = 0.3527$ nm). This suggests the presence of a jump-to-contact process similar to that seen when a nickel tip approaches a gold sample in AFM measurements [20].

After allowing the monolayers to approach to a distance at which the configurational energy reaches very high positive values we performed a second set of simulations by separating the monolayers using the same rate as that of the approach. The configurational energy results during the two approach stages and the separation stage are shown in Fig. 4. From both curves in Fig. 4, it can immediately be seen that there is hysteresis. The configurational energy during separation at intermediate and large distances is consistently lower than that during the approach stage. The maximum size of the difference is approximately kT between the potential minima, and is

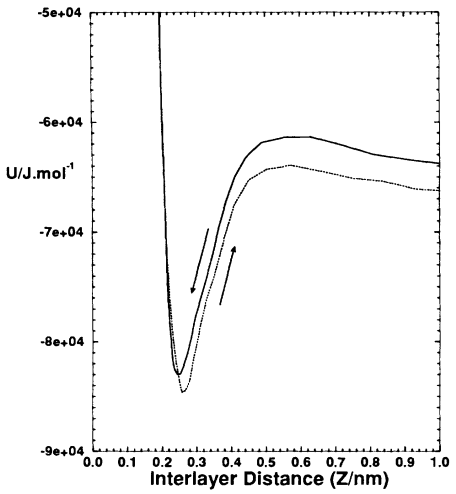

FIG. 4. Configurational energy of the total system U during approach and separation, as a function of the average interlayer distance Z.

comparable to a maximum hysteresis of $4kT$ as found by Yoshizawa, McGuiggan, and Israelachvili [3]. Similarly, direct force measurements show that the potential of mean force measured upon approach between two monolayers is different from that measured upon separation in adhesion experiments in which roughly the same coverage has been used to that used in our simulations [4,5]. The authors contend that hysteresis in approach-separation experiments, such as in adhesion between two plates, can be explained by the entanglement or interdigitation of molecules from different monolayers [4,5]. We believe that this is certainly true in the case of polymers [21,22], but is less likely in the case of molecules consisting of less than 20 carbons. In our simulations, no entanglements or interdigitation were observed between the monolayers; thus we believe that the hysteresis in the calculated configurational potential is due to the order-disorder phase transition. Such phase transitions are well known to exhibit hysteresis effects. This could also explain why Chaudhury and Owen observe hysteresis in adhesion experiments even for very dense monolayers in which entanglements are very unlikely [7]. Studies on the phase behavior of crystalline monolayers show that these undergo various order-disorder transitions such as tilting or rotator-nonrotator transitions [23].

In summary, our simulations predict that during some approach-separation experiments, such as in adhesion between two plates or friction between two adjacent surfaces, an order-disorder transition occurs which is responsible for hysteresis in calculated properties. Our results provide an additional explanation of the origin of hysteresis in approach-separation experiments. This order-disorder transition is less likely to occur at surface conditions such as density, pressure, and temperature that are far from conditions at which order-disorder transitions are expected in the free monolayers. Clearly, more simulations are needed to investigate the effects of compression rates on the simulation results. In particular, it would be crucial to investigate the effect of compression and expansion rates on the size of energy hysteresis.

A. van Helden, B. Smit, M. Phillips, J. I. Siepmann, and D. Cooper are gratefully acknowledged for useful discussions and comments on the manuscript.

[1] Y.-L. Chen, Z. Xu, and J. N. Israelachvili, Langmuir **8**, 2966 (1992).
[2] J. N. Glosli and G. M. McClelland, Phys. Rev. Lett. **70**, 1960 (1993).
[3] H. Yoshizawa, P. McGuiggan, and J. N. Israelachvili, Science **259**, 1305 (1993).
[4] J. N. Israelachvili, Vac. Sci. Technol. A **10**, 2961 (1992).
[5] H. Yoshizawa, Y.-L. Chen, and J. N. Israelachvili, J. Phys. Chem. **97**, 4128 (1993).
[6] Y.-L. Chen, C. A. Helm, and J. N. Israelachvili, J. Phys. Chem. **95**, 10736 (1991).
[7] M. K. Chaudhury and M. J. Owen, J. Phys. Chem. **97**, 5722 (1993).
[8] D. K. Schwartz, J. Garnaes, R. Viswanathan, and J. A. N. Zasadzinski, Science **257**, 508 (1992).
[9] S. Toxvaerd, J. Chem. Phys. **93**, 4290 (1990); P. Padilla and S. Toxvaerd, J. Chem. Phys. **94**, 5650 (1991); **95**, 509 (1991).
[10] P. van der Ploeg and H. J. C. Berendsen, J. Chem. Phys. **76**, 3271 (1982); Mol. Phys. **49**, 233 (1983).
[11] G. Cardini, J. P. Bareman, and M. L. Klein, Chem. Phys. Lett. **145**, 493 (1988); J. P. Bareman, G. Cardini, and M. L. Klein, Phys. Rev. Lett. **60**, 2152 (1988); J. P. Bareman and M. L. Klein, J. Phys. Chem. **94**, 5202 (1990).
[12] W. D. Luedtke and U. Landman, Comput. Mater. Sci. **1**, 1 (1992).
[13] J. T. Buontempo, S. A. Rice, S. Karaborni, and J. I. Siepmann, Langmuir **9**, 1604 (1993).
[14] J. I. Siepmann and I. McDonald, Phys. Rev. Lett. **70**, 453 (1993).
[15] S. Karaborni, Langmuir **9**, 1334 (1993).
[16] K. Kjaer, J. Als-Nielsen, C. A. Helm, P. Tippman-Krayer, and M. Möhwald, J. Phys. Chem. **93**, 3200 (1989).
[17] J. Hautman and M. L. Klein, J. Chem. Phys. **93**, 7483 (1990); **91**, 4994 (1989).
[18] D. Bloor, D. H. Bonsor, and D. N. Batchelder, Mol. Phys. **34**, 939 (1977).
[19] J. Doucet and A. J. Dianoux, J. Chem. Phys. **81**, 5043 (1984).
[20] U. Landman, W. D. Luedtke, N. A. Burnham, and R. J. Colton, Science **248**, 454 (1990).
[21] P. G. de Gennes, Adv. Colloid Interface Sci. **27**, 189 (1987).
[22] H. J. Taunton, C. Toprakcioglu, L. J. Fetters, and J. Klein, Science **332**, 712 (1988), and references therein.
[23] A M. Bibo, C. M. Knobler, and I. R. Peterson, J. Phys. Chem. **95**, 5591 (1991).

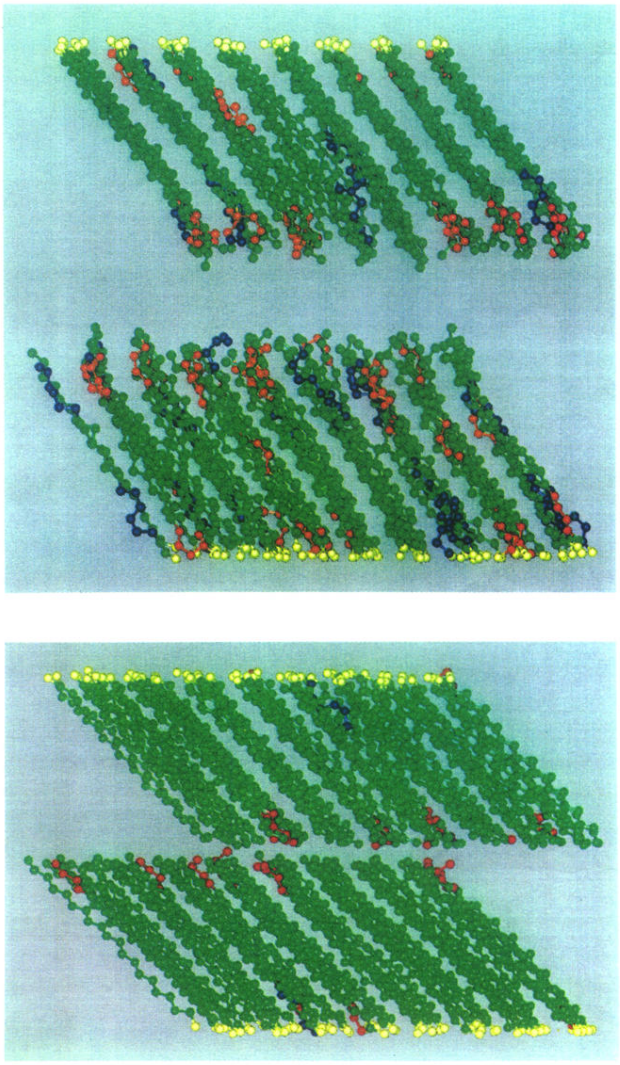

FIG. 3. Snapshots of the system at two interlayer distances: top: $Z = 0.938$ nm and bottom: $Z = 0.233$ nm. The headgroups are displayed in yellow and the methylene segments in green. Gauche defects separated from each other by more than one *trans* dihedral angle are displayed in red. Gauche defects separated from each other by exactly one *trans* dihedral angle (kink defects $g^{\pm}tg^{\mp}$) are displayed in blue.